NEOPLASIA
www.neoplasia.com

Volume 11 Number 12 December 2009 pp. 1272–1284 1272

Human Immunodeficiency Virus Type 1 Tat Accelerates Kaposi Sarcoma–Associated Herpesvirus Kaposin A–Mediated Tumorigenesis of Transformed Fibroblasts *In Vitro* as well as in Nude and Immunocompetent Mice[1]

Xiuying Chen[*,†,‡,§,¶,2], Lin Cheng[‡,#,2], Xuemei Jia[‡,2], Yi Zeng[,2], Shuihong Yao[‡], Zhigang Lv[‡], Di Qin[‡], Xin Fang[‡], Yongliang Lei[¶] and Chun Lu[*,†,‡,§]**

*Laboratory of Reproductive Medicine, Nanjing Medical University, Nanjing 210029, PR China; [†]Key Laboratory of Pathogen Biology of Jiangsu Province, Nanjing Medical University, Nanjing 210029, PR China; [‡]Department of Microbiology and Immunology, Nanjing Medical University, Nanjing 210029, PR China; [§]Key Laboratory for Laboratory Medicine of Jiangsu Province, Nanjing 210029, PR China; [¶]Lishui Center for Disease Control and Prevention, Lishui, Zhejiang, 323000, PR China; [#]Department of Microbiology and Immunology, Huanghe Science and Technology College, Zhengzhou 450006, PR China; **Department of Microbiology and Immunology, Youjiang Medical College for Nationalities, Bose 533000, PR China

Abstract

Kaposi sarcoma–associated herpesvirus (KSHV) is necessary but not sufficient to cause Kaposi sarcoma (KS). Coinfection with human immunodeficiency virus type 1 (HIV-1), in the absence of antiretroviral suppressive therapy, drastically increases the risk of KS. Previously, we identified that HIV-1 transactivative transcription protein (Tat) was an important cofactor that activated lytic cycle replication of KSHV. Here, we further investigated the potential of Tat to influence tumorigenesis induced by KSHV Kaposin A, a product of KSHV that was encoded by the open reading frame K12 (a KSHV-transforming gene). By using colony formation in soft agar, ^{3}H-TdR incorporation, cell cycle, and microarray gene expression analyses, we demonstrated that Tat enhanced proliferation as well as mitogen-activated protein kinase, signal transducer and activator of transcription 3, and phosphatidylinositol 3-kinase/protein kinase B signaling induced by Kaposin A in NIH3T3 cells. Animal experiments further demonstrated that Tat accelerated tumorigenesis by Kaposin A in athymic *nu/nu* mice. Cells obtained from primary tumors of nude mice succeeded inducing tumors in immunocompetent mice. These data suggest that Tat can accelerate tumorigenesis induced by Kaposin A. Our data present the first line of evidence that Tat may participate in KS pathogenesis by collaborating with Kaposin A in acquired immunodeficiency syndrome (AIDS)–related KS (AIDS-KS) patients. Our data also suggest that the model for Kaposin and Tat–mediated oncogenesis will contribute to our understanding of the pathogenesis of AIDS-KS at the molecular level and may even be important in exploring a novel therapeutic method for AIDS-KS.

Neoplasia (2009) 11, 1272–1284

Abbreviations: AIDS-KS, acquired immunodeficiency syndrome (AIDS)-related KS; Akt, protein kinase B; cpm, counts per minute; ERK, extracellular signal–regulated protein kinase; HIV-1, human immunodeficiency virus type 1; KS, Kaposi sarcoma; KSHV, Kaposi sarcoma–associated herpesvirus; PI3K, phosphatidylinositol 3-kinase; RT-PCR, reverse transcription–polymerase chain reaction; STAT3, signal transducer and activator of transcription 3; Tat, transactivative transcription protein; VEGF, vascular endothelial cell growth factor; vGPCR, viral G protein–coupled receptor

Address all correspondence to: Chun Lu, PhD, Department of Microbiology and Immunology, Nanjing Medical University, Nanjing 210029, PR China. E-mail: clu@njmu.edu.cn

[1]The authors thank the support from the National Natural Science Foundation of China (30670096 and 30972619 to C.L.; 30900064 to D.Q.), Fok Ying Tung Education Foundation (101038 to C.L.), Program for New Century Excellent Talents in University of China (NCET-05-0506 to C.L.), the Ministry of Science and Technology of Jiangsu Province (BK2006524 to C.L.), Program for Changjiang Scholars and Innovative Research Team in University of China (IRT0631), and the Ministry of Health of Jiangsu Province (no. XK200731).

[2]The first four authors contributed equally to this work.

Received 18 March 2009; Revised 18 May 2009; Accepted 26 May 2009

DOI 10.1593/neo.09494

Introduction

Kaposi sarcoma–associated herpesvirus (KSHV, also designated human herpesvirus 8 or HHV-8) has been causally linked to the development of Kaposi sarcoma (KS) [1]. The KS lesions are characterized by proliferating spindle cells, prominent angiogenesis, hemorrhage, and leukocyte infiltration. Although KSHV is necessary for the development of KS, other factors may also play important roles in the pathogenesis of this disease. One potentially important cofactor is human immunodeficiency virus type 1 (HIV-1). Individuals dually infected with KSHV and HIV-1 have a greatly enhanced prevalence of KS compared with those infected with KSHV alone [2]. Immune dysfunction likely accounts for some of the increased incidence of KS in double infections, but it may not be the sole contributing factor. For instance, studies indicated that KS developed almost exclusively in HIV-1–positive, but not HIV-2–positive, patients in Gambia, West Africa, despite essentially equivalent seroprevalence for KSHV and severity of immunosuppression in both groups of patients [3]. In addition, acquired immunodeficiency syndrome (AIDS)–related KS (AIDS-KS) has a more aggressive course than other forms of KS, including those associated with iatrogenic immunosuppression in transplant patients. Therefore, studies have continued to focus on other mechanisms, such as induction of cytokine expression and production of HIV-1–encoded proteins, particularly the secreted HIV-1 protein, transactivative transcription protein (Tat). Previous studies indicated that Tat acted as a growth factor for KS-derived endothelial cells [4,5], possibly in part through synergy with or dysregulation of the expression of proinflammatory cytokines [6–9]. Recently, we showed that Tat was an important cofactor that activated lytic cycle replication of KSHV by modulating Janus kinase (JAK)/signal transducer and activator of transcription (STAT) signaling [10]. Thus, Tat promotes tumorigenesis of endothelial cells, both through stimulation of vascular endothelial growth factors, antiapoptotic activity, and KSHV replication [11]. These data suggest a role of Tat in the pathogenesis of AIDS-KS.

KSHV genome contains open reading frames (ORFs) to code for 81 proteins, of which 66 are similar to other γ-herpesviruses and 15 are unique to KSHV. There are six genes that have been shown to possess oncogenic properties in cell culture. They are *ORF K1* (a glycoprotein), *ORF K9* (a viral interferon-regulatory factor), *ORF74* (a viral G protein–coupled receptor or vGPCR), *ORF73* (latency-associated nuclear antigen), *ORF72* (viral cyclin), and *ORF K12* (Kaposin). The first three genes are transcribed during the lytic phase of KSHV replication, and the rest are expressed during latency [12]. Specifically, Kaposin is expressed from T0.7 transcripts in latently infected cells, and messenger RNA (mRNA) can be detected in earliest to advanced stages of KS lesions [13–15]. Studies demonstrated that the initiation of transcription at the *K12* locus is complex, with multiple transcripts of various lengths being produced resulting in Kaposin A, B, and C forms with molecular weights of 6.6, 38, and 54 kDa, respectively [16]. Because Kaposin A is the predominant form in KSHV-infected cells, several groups have used this form to investigate the transformation properties of this protein. It was demonstrated that Kaposin A induced transformation of Rat-3 cells [17]. These transformed cells induced highly angiogenic, undifferentiated sarcomas in athymic nude mice within 1 to 3 weeks [17].

Although the mechanisms of KS pathogenesis by KSHV are not fully elucidated, an increasing body of evidence suggests that the vGPCR plays an important role. It induces angiogenesis and vascular endothelial growth factor (VEGF) expression *in vitro* and *in vivo* in mice, and transgenic mice expressing vGPCR develop angioproliferative lesions with many of the characteristics of KS [18–21]. Interestingly, by inducing activation of nuclear factor of activated T cells (NF-AT) and nuclear factor-kappaB (NF-κB), Tat can accelerate tumorigenesis by vGPCR [22]. Thus, these facts led us to hypothesize that Tat may participate in pathogenesis of AIDS-KS by influencing Kaposin A–mediated tumorigenesis.

Therefore, we have explored the possible role of HIV-1 Tat in Kaposin-A–induced NIH3T3 cell proliferation *in vitro*/tumorigenesis in athymic *nu/nu* and immunocompetent mice.

Materials and Methods

Cells, Plasmids, and Transfection

NIH3T3 cells were maintained in Dulbecco's modified Eagle's medium (DMEM) containing 10% heat-inactivated fetal bovine serum, 2 mM L-glutamine, 100 U/ml penicillin, and 100 μg/ml streptomycin (complete medium) at 37°C in a humidified, 5% carbon dioxide atmosphere. To express KSHV–Kaposin A in NIH3T3 cells, a 169-bp fragment of KSHV *ORF K12* was obtained from BCBL-1 cells by polymerase chain reaction (PCR) [17] and inserted into the pcDNA3.1 plasmid vector (Invitrogen, Inc, Carlsbad, CA). To express HIV-1–Tat in NIH3T3 cells, the pTat101 plasmid was used as described previously [10]. The dominant-negative STAT3 construct (pMSCV-STAT3D-EGFP, designated as STAT3-DN in this study) was kindly provided by Dr. D. Link (Washington University School of Medicine, MO) [23]. Transfections were performed with Lipofectamine 2000 reagent (Invitrogen). Transfected cells were selected in G418 (Life Technologies, Gaithersburg, MD), and resistant colonies were isolated after 2 to 3 weeks. Stable transfectant colonies were cloned by end point limiting dilution.

Reverse Transcription–PCR

Reverse transcription–PCRs (RT-PCRs) were performed as described previously [24]. Primers used for analysis in this study are listed in Table 1.

Table 1. Sets of Primers Used in RT-PCR*.

mRNA	Oligonucleotides	Accession No.	Expected Size (bp)	Annealing Temperature (°C)	Cycles
KSHV K12	F: 5′-ATG GAT AGA GGC TTA ACG GTG T-3′ R: 5′-TTG CAA CTC GTG TCC TGA ATG-3′	NC_003409	169	56	35
HIV-1 Tat	F: 5′-ATG GCA GGA AGA AGC GGA GAC-3′ R: 5′-GTC GTC CTT GTA GTC GCC TC-3′	NC_001802	186	56	35
β-Actin†	F: 5′-TGA CGG GGT CAC CCA CAC TGT GCC CAT CTA-3′ R: 5′-CTA GAA GCA TTT GCG GTG GAC GAT GGA GGG-3′	BC016045	661	56	19

F indicates forward; *R*, reverse.
*The oligonucleotides were selected from the sequences with the indicated accession number. The size of each amplified product, its annealing temperature, and numbers of PCR cycles are indicated.
†These genes belong to human genome.

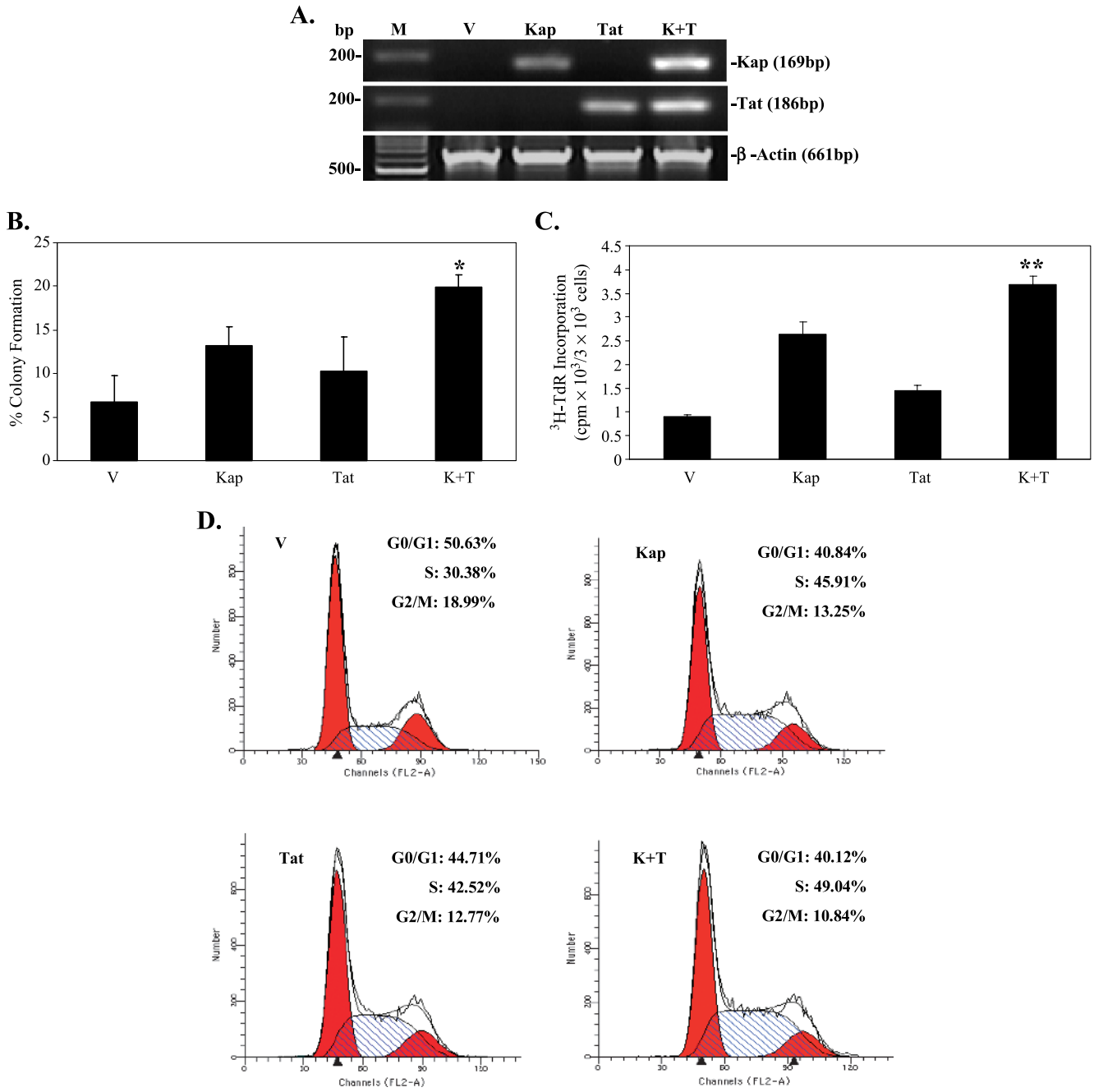

Figure 1. Tat enhances proliferation of Kaposin A–transformed NIH3T3 cells. (A) RT-PCR analysis for Kaposin A and Tat mRNA in stable transfectant colonies of NIH3T3 cells. Kaposin A and Tat mRNA expression in pcDNA3.1 vector (V), Kaposin A (Kap), Tat (Tat), or Kaposin A plus Tat (K + T) stable transfectant colonies of NIH3T3 cells were detected by RT-PCR. M represents DNA molecular marker, and β-actin was readily detectable in all samples indicating the presence of amplifiable complementary DNA. (B) Quantitation of soft agar colony formation of four transfectants. After 21 days in culture, colony formation was scored by estimating the total number of colonies with a diameter greater than 0.1 mm present in triplicate wells for pcDNA3.1 vector (V), Kaposin A (Kap), Tat (Tat), or Kaposin A plus Tat (K + T) transfectant colonies of NIH3T3 cells. The results are expressed as the mean ± SD ($n = 3$). *$P < .05$ for Student's *t*-test *versus* Kap and Tat groups, respectively. (C) The ^{3}H-TdR incorporation assay for cell proliferation detection of four transfectants. After serum starving for 24 hours, the pcDNA3.1 vector (V), Kaposin A (Kap), Tat (Tat), or Kaposin A plus Tat (K + T) transfectants of NIH3T3 cells were cultured in complete medium for 72 hours and labeled for the last 12 hours with ^{3}H-TdR. The cells were collected, and the radioactivity was measured by liquid scintillation counter. Data were expressed as the cpm of mean ± SD ($n = 3$). **$P < .01$ for Student's *t*-test *versus* Kap and Tat groups, respectively. (D) Flow cytometric analysis for cell cycle characteristics of four transfectants. After serum starving for 24 hours, the pcDNA3.1 vector (V), Kaposin A (Kap), Tat (Tat), or Kaposin A plus Tat (K + T) transfectants of NIH3T3 cells were continued to culture in complete medium for 16 hours, then harvested and washed with PBS. The cell suspensions were treated and stained with propidium iodide followed by flow cytometric analysis for cell cycle distribution. A representative experiment is shown. The first peak corresponds to cells in G_0/G_1-phase, the intermediary population to cells in S-phase, and the second peak corresponds to cells in the G_2/M-phase. Very similar findings were observed in two repeat experiments.

Soft Agar Assay

For analysis of colony formation, cell suspensions containing 0.3% agar were seeded in each well of 24-well plates containing an underlay of 0.6% agar in complete medium. Cultures were supplemented with complete medium per week and colonies were scored 21 days after seeding the cells.

Proliferation Assay

For the ^{3}H-TdR incorporation, serum-starved cells were cultured in complete medium for 72 hours and labeled for the last 12 hours with 1 μCi of [^{3}H]thymidine (^{3}H-TdR; Institute of Radionuclide of China, Beijing). Then, the cells were collected, and the radioactivity was measured by liquid scintillation counter (Beckman, Fullerton, CA). All the experiments were repeated independently at least three times on 96-well plates, and triplicate wells were used. The data represent the mean counts per minute (cpm).

Flow Cytometry

After serum starving for 24 hours, cells continued to culture in complete medium for 16 hours, then were harvested and washed three times with PBS by centrifugation at 1000*g* for 5 minutes to remove cell debris. The cell suspensions were fixed in ice-cold 75% ethanol for 24 hours at −20°C. The samples were washed and resuspended in PBS and then treated with 1% (vol/vol) Triton X-100 and 10 mg/ml RNase A for 10 minutes at 37°C. Staining of cellular DNA was performed with 20 mg/ml propidium iodide for 20 minutes at room temperature in the dark. The percentage of the cells in the G_0/G_1, S, and G_2/M phases in the cell cycle were immediately analyzed by Flow Cytometry (Coulter Becton-Dickinson, Miami, FL).

Antibodies

Anti-STAT3 rabbit polyclonal antibody (pAb), anti-VEGF rabbit pAb, horseradish peroxidase–conjugated goat antimouse and antirabbit immunoglobulin G were purchased from Santa Cruz Biotechnologies (Santa Cruz, CA). Anti–phospho-STAT3 (Tyr705) rabbit monoclonal antibody (mAb), anti–cyclin D1 rabbit mAb, anti–phospho–extracellular signal–regulated protein kinase 1/2 (ERK1/2; Thr202/Tyr204) rabbit pAb, anti–phospho-MEK1/2 (Ser217/221) rabbit pAb, anti–phospho phosphatidylinositol 3-kinase (PI3K) [p85(Tyr458)/p55(Tyr199)] rabbit pAb, anti–phospho-Akt (Ser473) mouse mAb, and anti–Survivin rabbit mAbs were obtained from Cell Signaling Technologies (Danvers, MA). Anti–Akt rabbit pAbs were purchased from BioVision Incorporated (Mountain View, CA). Anti–ERK1/2 rabbit pAb were obtained from KangChen Bio-tech (Shanghai, China). Mouse mAbs to β-actin (Boster Technologies, Wuhan, Hubei, China) were used to monitor sample loading.

Western Blot Analysis

After serum starving for 24 hours, cells were harvested and lysed in rapid immunoprecipitation assay buffer containing a phosphatase inhibitor cocktail and protease inhibitors. Protein concentration was determined using a Bradford Assay (Bio-Rad Laboratories, Hercules, CA). Western blot analyses were performed as described previously [25,26].

Tumorigenicity Assay

Animal care and handling conformed to the Guide for Care and Use of Laboratory Animals published by the US National Institutes of Health, and the study was approved by Nanjing Medical University's ethical committee. The tumorigenic potential of stable transfectant cells and cells isolated from induced tumor was tested in 3- to 4-week-old male athymic BALB/c *nu/nu* mice (Shanghai Slac Laboratory Animal Center, Shanghai, China) and 3- to 4-week-old male BALB/c immunocompetent mice (Laboratory Animals Center, Medical School of Yangzhou University, Yangzhou, China), respectively, both of which were housed under specific pathogen-free conditions. Stable transfectant cells (2×10^6 cells per 200 μl of PBS per animal) were injected subcutaneously (s.c.) behind the neck. Five mice were used in each group, and experiments were performed twice. The nude mice were monitored every day for the appearance of tumors. Tumor size was estimated as the product of two-dimensional caliper measurements. Tumor-bearing mice were killed, and tumors were formalin-fixed and paraffin-embedded in their entireties. In addition, the tumors were minced, digested with 0.1% collagenase, and cultured in DMEM. Medium was changed every 3 days for 2 to 3 weeks with fresh medium containing G418. After reaching confluence, G418-resistant cells were analyzed for Tat, Kaposin A expression by RT-PCR. Then, the cells were injected s.c. into the right flanks of BALB/c immunocompetent mice (2×10^6 per cells per 200 μl of PBS per animal), and 10 mice were used in each group. The mice were monitored every day for the appearance of tumors, and tumor size was estimated as described above.

Immunohistochemistry

Informative sections of formalin-fixed, paraffin-embedded tumor from athymic BALB/c *nu/nu* mice were immunostained as described elsewhere [27].

SuperArray Analysis

SuperArray analysis of gene expression was performed according to the manufacturer's directions (GEArray Q series Kit nonradioactive; SuperArray, Inc, Bethesda, MD) and as described previously [10].

Statistical Analysis

All experiments were performed at least in triplicate. Numerical data were expressed as mean ± SD. Two group comparisons were analyzed by two-sided Student's *t*-test. *P* values were calculated, and $P < .05$ was considered significant.

Results

Tat Enhances Proliferation of Kaposin A–Transformed NIH3T3 Cells

To generate stable transfectants, we transfected Kaposin A, Tat, and Kaposin A plus Tat constructs into NIH3T3 cells. Stable transfectants were selected, and expressions of target genes were examined by RT-PCR. The mRNA of Kaposin A was readily expressed in Kaposin A alone or Kaposin A plus Tat–transfected NIH3T3 cells. Also, Tat mRNA was expressed in Tat alone or in Kaposin A plus Tat–transfected NIH3T3 cells (Figure 1*A*).

KSHV *ORF K12* coding for Kaposin A has been identified as a transforming gene, which could induce not only cell proliferation *in vitro* but also tumor formation *in vivo* [17]. To determine whether Tat can influence NIH3T3 cells proliferation by Kaposin A, colony formation assay was performed. As shown in Figure 1*B*, the percentage of colony formation of Kaposin A plus Tat transfectants in NIH3T3 cells was increased 1.51- ($P < .05$) and 1.94-fold ($P < .05$) compared with those of Kaposin A and Tat transfectants, respectively. The ^{3}H-TdR incorporation assay also demonstrated that Tat further enhanced proliferation of Kaposin-transformed cells. As we could see in Figure 1*C*, the cpm

Table 2. Expression of Gene Indicators for the Activation of 15 Different Signal Pathways Involved in Oncogenesis in Kaposin A–, Tat-, or Kaposin A Plus Tat–transfected NIH3T3 Cells and These Cells Induced Tumor in Nude Mice.

Gene Function and Name	Accession No.	Fold Change When Compared with pcDNA3.1-Transfected NIH3T3 Cells (*In Vitro*) or pcDNA3.1-Transfected NIH3T3 Cells–Induced Tumor (*In Vivo*)					
		In Vitro			*In Vivo*		
		Kaposin A	Tat	K + T	Kaposin A	Tat	K + T
Androgen pathway							
Cdk 2L	NM_016756	1.47	0.82	0.85	1.11	1.36	0.96
$p21^{Waf1}$/$p21^{cip}$	NM_007669	1.22	1.48	1.09	2.16	0.65	1.52
EGFR	NM_007912	1.25	1.55	4.34	1.66	0.81	2.93
Folh1	NM_016770	1.68	1.69	4.49	0.54	0.88	1.02
Kallikrein 3	NM_008455	2.55	2.02	2.81	1.51	0.51	2.14
N4wbp4T/MEPAI	NM_022995	1.08	1.22	1.59	1.02	1.13	1.81
Ngfa	NM_010915	N/A	N/A	N/A	2.65	0.77	2.51
Cox-2 pathway							
c-fos	NM_010234	1.07	1.57	3.86	1.39	0.81	3.46
Hspa4	NM_008300	0.89	1.29	1.5	0.49	0.74	1.16
Mcl-1	NM_008562	1.35	1.52	1.92	0.43	0.72	1.14
Pparg	NM_011146	1.73	1.19	1.82	6.86	17.77	2.16
Cox-2	NM_011198	1.38	1.11	4.28	0.52	0.41	0.66
TRAIL-R/DR5	NM_020275	1.32	0.27	0.73	1.74	3.99	1.57
DNA damage/p53 pathways							
$p21^{Waf1}$/$p21^{cip}$	NM_007669	1.22	1.48	1.09	2.16	0.65	1.52
Hspa4	NM_008300	0.89	1.29	1.5	0.49	0.74	1.16
Bax	NM_007527	0.81	1.89	2.48	2.52	0.7	1.47
Bcl-2	NM_009741	0.81	2.14	2.34	2.74	1.29	3.17
Gadd45	NM_007836	5.82	5.28	5.09	0.82	2.22	0.91
Hif1a	NM_010431	1.25	1.16	1.55	0.44	0.59	0.64
Igfbp3	NM_008343	2.15	3.4	7.13	0.89	0.7	1.84
Mdm2	NM_010786	0.88	1.32	1.37	0.81	0.9	1.39
Fas	NM_007987	0.44	0.33	0.33	2.52	0.76	2.75
Trail	NM_009425	1.57	0.68	2.89	0.82	0.35	0.31
TRAF1	NM_009421	1.28	1.46	1.74	1.02	1.18	1.13
Wig1	NM_009517	1.51	1.96	2.44	0.9	0.8	1.01
Estrogen pathway							
EGFR	NM_007912	1.25	1.55	4.34	1.66	0.81	2.93
Bcl-2	NM_009741	0.81	2.14	2.34	2.74	1.29	3.17
BRCA1	NM_009764	0.57	1.49	4.44	1.64	0.95	2.4
Cathepsin D	NM_009983	1.02	1.27	0.87	0.34	0.96	0.76
Progesterone receptor	NM_008829	4.9	3.93	11.36	2.36	0.58	2.07
EFP/Zfp147	D63902	1.91	1.87	4.24	1.62	1	1.76
Hedgehog pathway							
BMP2	NM_007553	3.82	3.5	5.96	5.42	0.78	5.91
BMP4	NM_007554	0.57	1.83	4.04	2.4	0.84	4.19
HNF3B/forkhead box A2	NM_010446	0.97	1.48	4.52	1.58	0.89	2.37
Hip	NM_020259	2.62	1.94	3.13	0.68	0.8	0.76
Patched	NM_008957	1.59	0.84	3.11	3.84	4.07	7.82
Patched 2	NM_008958	1.12	0.37	0.71	1.58	1.07	2.26
Wnt1	NM_021279	3.17	2.04	5.83	1.22	0.93	0.97
Wnt2	NM_023653	2.27	2	5.75	1.78	0.64	1.54
WSB-1	NM_019653	1.47	1.09	2.24	0.46	0.87	0.65
Hypoxia pathway							
$p21^{Waf1}$/$p21^{cip}$	NM_007669	1.22	1.48	1.09	2.16	0.65	1.52
Igfbp3	NM_008343	2.15	3.4	7.13	0.89	0.7	1.84
Edn1	NM_010104	0.45	1.36	1.54	1.31	0.92	3.12
Epo	NM_007942	2.79	2.71	3.77	1.42	0.69	1.06
Hk1	NM_010438	1.62	1.78	2.07	1.14	0.72	1.13
HMOX1	NM_010442	1.01	1.09	0.95	0.81	0.88	1.02
iNOS	NM_010927	3.85	2.84	11.97	2.58	0.83	2.61
Glucose transporter 1	NM_011400	1.43	1.35	1.78	0.78	0.99	1.61
Transferrin	NM_133977	2.89	2.06	4.92	1	0.96	1.03
Tfr1	NM_011638	0.98	0.93	1.06	0.35	0.89	0.81
VEGF/VEGI	NM_009505	0.99	0.84	1.7	0.76	1.16	1.01
Inflammation/NF-κB pathways							
iNOS	NM_010927	3.85	2.84	11.97	2.58	0.83	2.61
ICAM-1	NM_010493	2.21	2.09	4.99	1.26	0.76	2.29
IL-2	NM_008366	0.85	1.2	1.17	0.83	0.86	1.29
TNFb	NM_010735	5.71	4.33	10.65	1.46	0.55	1.31
NFkB1	NM_008689	3.22	2.17	4.52	2.13	0.74	2.69
ikBa/Mad3	NM_010907	2.13	2.17	2.93	1.52	1.18	1.63
TNFa	NM_013693	4.73	3.83	15.54	1.49	0.56	1.92
VCAM-1	NM_011693	0.97	0.82	2.16	1.41	4.29	2.1

Table 2. (*continued*)

Gene Function and Name	Accession No.	Fold Change When Compared with pcDNA3.1-Transfected NIH3T3 Cells (*In Vitro*) or pcDNA3.1-Transfected NIH3T3 Cells–Induced Tumor (*In Vivo*)					
		In Vitro			*In Vivo*		
		Kaposin A	Tat	K + T	Kaposin A	Tat	K + T
Mitogen-activated protein kinase pathway							
c-fos	NM_010234	1.07	1.57	3.86	1.39	0.81	3.46
Cola1	NM_007742	1.22	1.07	0.87	0.47	1.07	0.94
Krox-24	NM_007913	31.9	14.18	3.75	0.8	2.57	1.55
c-JUN	NM_010591	1.41	1.79	2.43	0.94	1.16	2.33
PI3K/Akt pathways							
Bcl-2	NM_009741	0.81	2.14	2.34	2.74	1.29	3.17
Hif1a	NM_010431	1.25	1.16	1.55	0.44	0.59	0.64
Trail	NM_009425	1.57	0.68	2.89	0.82	0.35	0.31
c-JUN	NM_010591	1.41	1.79	2.43	0.94	1.16	2.33
Cyclin D1	NM_007631	1.02	0.7	0.98	0.95	1.32	0.98
Fn1	XM_129845	1.05	1.34	0.98	0.8	0.79	0.84
MMP7	NM_010810	2.32	1.05	1.07	0.64	21.65	1.46
c-myc	NM_010849	1.49	1.06	2.94	1.12	2.81	1.61
STAT pathway							
Bcl-2	NM_009741	0.81	2.14	2.34	2.74	1.29	3.17
iNOS	NM_010927	3.85	2.84	11.97	2.58	0.83	2.61
Bcl-x	NM_009743	1.22	4.14	10.84	3.4	1.36	4.1
Beta-casein	NM_009972	2.81	2.52	3.42	1.45	0.59	0.94
MIG/Scyb9	NM_008599	1	1.91	2.68	2.95	0.95	2.61
IL-4	NM_021283	1.36	1.63	4.22	1.23	0.17	2.22
IL-4R	NM_010557	6.68	1.57	2.4	0	4.44	0.1
IRF-1	NM_008390	0.98	1.27	0.99	0.14	1.89	1.03
Stromelysin 2	NM_019471	8.03	6.11	22.7	3.23	2.98	3.89
A1m	NM_007376	5.95	3.33	10.52	1.63	0.51	1.38
Stress/heat shock pathways							
Hspa4	NM_008300	0.89	1.29	1.5	0.49	0.74	1.16
Hsf1 (tcf5)	NM_008296	1.06	1.35	2.9	0.62	0.54	1.65
Hsp25	NM_013560	6.68	4.7	4.28	0.79	1.73	1.07
Hspb2	NM_024441	1.02	1.07	0.96	0.9	0.92	0.94
Hsp86-1	NM_010480	0.88	1.01	0.92	0.61	0.84	0.82
Stress/p38 and JNK pathways							
c-fos	NM_010234	1.07	1.57	3.86	1.39	0.81	3.46
Hspa4	NM_008300	0.89	1.29	1.5	0.49	0.74	1.16
Cola1	NM_007742	1.22	1.07	0.87	0.47	1.07	0.94
c-myc	NM_010849	1.49	1.06	2.94	1.12	2.81	1.61
Hsp25	NM_013560	6.68	4.7	4.28	0.79	1.73	1.07
Hspb2	NM_024441	1.02	1.07	0.96	0.9	0.92	0.94
ABCB4	NM_011076	0.9	0.82	0.82	9.5	4.13	9.69
ABCB1	NM_011075	1.04	0.81	0.68	3.23	1.44	4.86
CRE-BP/Creb2	NM_009715	1.4	1.51	1.5	0.81	0.93	2.09
Ptpn16	NM_013642	0.69	1.07	0.74	1.04	0.89	2.39
autotaxin (ATX)	NM_015744	3.43	2.41	2.76	0.93	0.97	1.11
grp78	NM_022310	0.73	1.03	1.25	0.31	0.85	0.95
p53	NM_011640	1.74	0.83	2.44	5.56	9.97	1.06
Survival/NF-κB pathway							
TRAF1	NM_009421	1.28	1.46	1.74	1.02	1.18	1.13
Bcl-x	NM_009743	1.22	4.14	10.84	3.4	1.36	4.1
AKT-1	NM_009652	1.14	1.41	0.74	1.74	0.79	4.05
Bfl-1	NM_007536	0.57	2.62	6.14	1.28	1.56	1.6
NAIP1	NM_008670	0.92	0.43	0.44	2.46	2.92	2.96
NAIP2	NM_010872	1.05	0.67	0.72	2.32	1.3	2.02
NAIP5	NM_010870	0.94	1.17	0.78	1.23	1.25	1.39
IAP1	NM_007464	3.28	2.03	1.63	3.01	0.66	2.03
IAP2	NM_007465	1.38	3.84	5.8	2.3	1.9	1.38
TNFAIP3	NM_009397	1.87	0.26	1.77	N/A	N/A	N/A
TGF-β pathway							
$p21^{Waf1}/p21^{cip}$	NM_007669	1.22	1.48	1.09	2.16	0.65	1.52
$p27^{Kip1}$	NM_009875	1.52	2.85	1.52	2.06	0.79	1.84
$p57^{Kip2}$	NM_009876	1.04	1.96	2.46	3.32	0.89	1.91
$p16^{ink4a}$	NM_009877	0.64	1.45	1.73	1.65	0.98	2.39
$p15^{INK4b}$	NM_007670	0.83	1.32	1.45	1.02	0.79	1.43
p18	NM_007671	0.92	1.2	1.33	0.79	0.97	1.13
p19	NM_009878	2.79	1.42	1.56	1.09	1.42	1.64
Wnt pathway							
BMP 4	NM_007554	0.57	1.83	4.04	2.4	0.84	4.19
VEGF/VEGI	NM_009505	0.99	0.84	1.7	0.76	1.16	1.01

Table 2. (*continued*)

Gene Function and Name	Accession No.	Fold Change When Compared with pcDNA3.1-Transfected NIH3T3 Cells (*In Vitro*) or pcDNA3.1-Transfected NIH3T3 Cells–Induced Tumor (*In Vivo*)					
		In Vitro			*In Vivo*		
		Kaposin A	Tat	K + T	Kaposin A	Tat	K + T
c-JUN	NM_010591	1.41	1.79	2.43	0.94	1.16	2.33
Cyclin D1	NM_007631	1.02	0.7	0.98	0.95	1.32	0.98
MMP7	NM_010810	2.32	1.05	1.07	0.64	21.65	1.46
c-myc	NM_010849	1.49	1.06	2.94	1.12	2.81	1.61
ABCB4	NM_011076	0.9	0.82	0.82	9.5	4.13	9.69
ABCB1	NM_011075	1.04	0.81	0.68	3.23	1.44	4.86
autotaxin (ATX)	NM_015744	3.43	2.41	2.76	0.93	0.97	1.11
Fra1	NM_010235	0.78	1.25	1.9	1.14	1.13	2.34
ID2	NM_010496	1.15	1.27	1.24	0.84	0.94	1.21
Tcf1	NM_009327	5.17	3.65	12.01	1.13	0.65	1.67
ELM1	NM_018865	2.08	2.1	2.84	0.67	1.17	0.77

of Kaposin A plus Tat transfectants in NIH3T3 cells was increased 1.4-($P < .01$) and 2.54-fold ($P < .01$) compared with those of Kaposin A and Tat transfectants, respectively. To further support this, cell cycle profiles analysis showed that the control vector transfectant contained approximately 30% of the cells in S-phase, whereas Kaposin A transfectant was observed with approximately 46% of the cells in S-phase. A similar profile was seen with Tat transfectant with approximately 43% of the cells in S-phase. Notably, Kaposin A plus Tat transfectant had a slightly high proportion (approximately 50%) of cells in S-phase (Figure 1*D*). Together, these data suggest that Tat may enhance NIH3T3 cells proliferation medicated by Kaposin A.

Tat Increases the MEK/ERK, STAT3, and PI3K/Akt Signals by Kaposin A

To detect which signaling pathways were activated by Tat in Kaposin A–transduced NIH3T3 cells, we first detected gene expressing profile changes affected by Kaposin A and/or Tat using microarray technique. The Q Series signal transduction gene array in mouse cancer, which

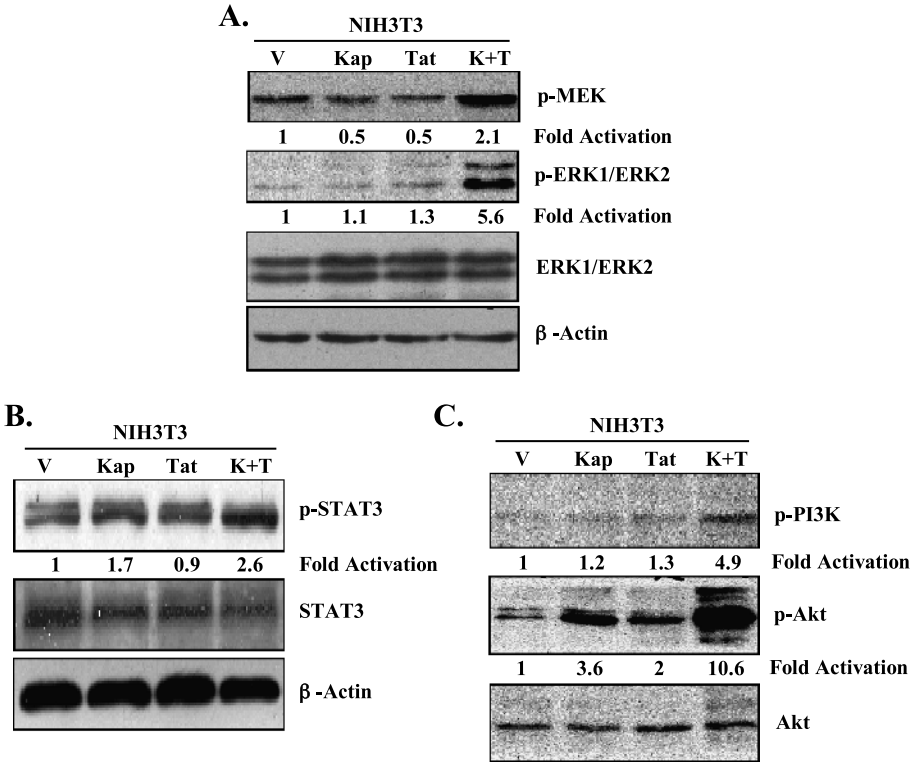

Figure 2. Enhanced activation of MEK/ERK, STAT3, and PI3K/Akt signals by Kaposin A and Tat in combination. (A, B, C) Activation of MEK/ERK (A), STAT3 (B), and PI3K/Akt (C) signals in Kaposin A plus Tat–transfected NIH3T3 cells. After serum starving for 24 hours, the pcDNA3.1 vector (V), Kaposin A (Kap), Tat (Tat), and Kaposin A plus Tat (K + T) transfectants of NIH3T3 cells were harvested and lysed in RIPA buffer containing a phosphatase inhibitor cocktail and protease inhibitors. Lysates were subjected to SDS-PAGE, transferred to membrane then immunoblotted with the indicated anti–phospho antibody. The membrane was stripped and reprobed with respective antibody or with antiactin to confirm the equal amounts of protein in each sample. The phosphorylation levels in V group were considered to be 1 for comparison.

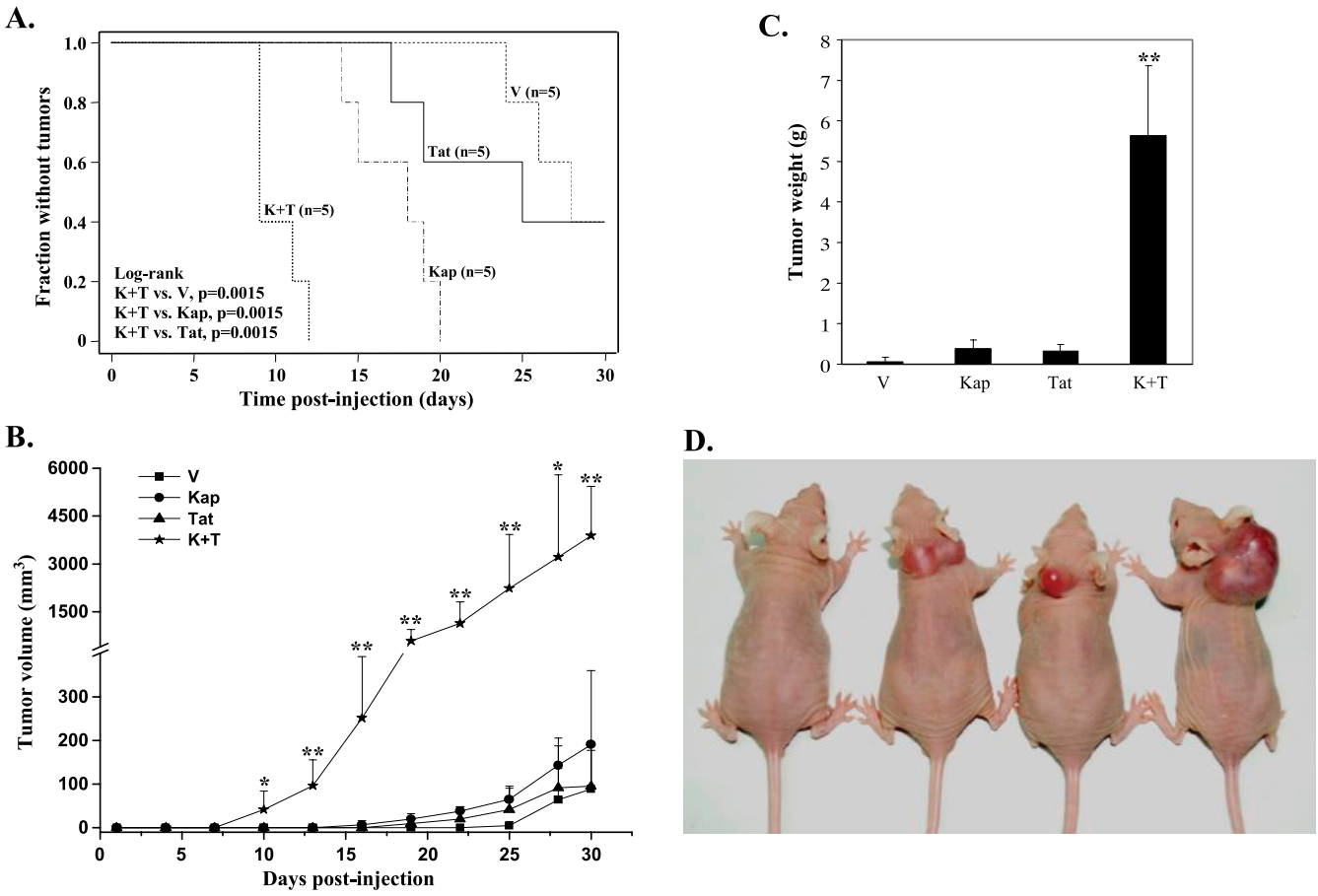

Figure 3. Tat accelerates tumorigenesis medicated by Kaposin A in BALB/c *nu/nu* mice. Tumors were induced by s.c. injection with the pcDNA3.1 vector- (V), Kaposin A– (Kap), Tat- (Tat), and Kaposin A plus Tat– (K + T) transfected NIH3T3 cells in nude mice as described in Materials and Methods. (A) A Kaplan-Meier plot for the time of appearance of palpable tumors is shown. A log-rank analysis gave a *P* value of .0015 for the comparison of K + T with Kap, Tat and control vector, and a *P* value of .0018 for the comparison of Kap with control vector. The log-rank *P* values were .6654 for the comparison of Tat with vector and .0581 for the Kap with Tat, indicating that there were no significant differences between these groups. (B) Plot of the volume of the tumors. The results are expressed as the mean ± SD ($n = 5$). $^{*}P < .05$ and $^{**}P < .01$ for Student's *t*-test *versus* Kap and Tat groups, respectively. (C) Column diagram of average tumor weight. Tumor-bearing mice were killed at day 30 after injections, and tumors were removed and weighed. Data reflect the mean ± SD. $^{**}P < .01$ for Student's *t*-test *versus* Kap and Tat groups, respectively. (D) Representative mice at day 30 after injections with V-, Kap-, Tat-, and K + T–transfected NIH3T3 cells, respectively, from left to right.

profiles the expression of 113 gene indicators or markers belonging to 15 different signal pathways involved in oncogenesis, was used to screen the potential signal pathway(s). As shown in Table 2, mRNA of many gene markers of 15 different signal pathways in Kaposin A, Tat, and Kaposin A plus Tat–transfected NIH3T3 cells were altered to some degree compared with control vector–transfected NIH3T3 cells. Noteworthy, mRNA of majority gene markers from mitogen-activated protein kinase and STAT pathways were consistently increased more than two-folds in Kaposin A plus Tat–transfected NIH3T3 cells compared with the corresponding controls (Table 2). To further examine whether these pathways are really activated in Kaposin A plus Tat–transfected NIH3T3 cells, Western blot were performed. We found that both Kaposin A and Tat alone failed to increase phosphorylated forms of MEK and ERK in NIH3T3 cells. However, their combination (Kaposin A plus Tat) significantly elevated phosphorylation levels of these two proteins (Figure 2*A*). Similarly, activation of STAT3 was significantly enhanced in both Kaposin A and Kaposin A plus Tat–transfected NIH3T3 cells, although Tat alone did not elevate phosphorylated STAT3 when compared with the corresponding control (Figure 2*B*). Because the PI3K/Akt pathway was involved in cell proliferation and tumor formation [28,29], we therefore measured protein expression of PI3K and Akt. Neither Kaposin A nor Tat alone upregulated phosphorylated PI3K level. However, both Kaposin A and Tat effectively elevated phosphorylated Akt in NIH3T3 cells. Interestingly, we again found that Kaposin A and Tat in combination in NIH3T3 cells significantly increased both PI3K and Akt phosphorylation levels, particularly for Akt. The increase was up to more than 10 folds compared with the vector control (Figure 2*C*). Actually, the data from microarray showed that half of mRNA of gene markers from PI3K/Akt pathway were increased in Kaposin A plus Tat–transfected NIH3T3 cells compared with the corresponding controls (Table 2).

These data collectively suggest that Tat increases activation of the MEK/ERK, STAT3, and PI3K/Akt signals by Kaposin A.

Tat Accelerates Tumorigenesis Mediated by Kaposin A in Nude Mice

To further test whether Tat could influence tumorigenesis induced by Kaposin A *in vivo*, we injected the transformed NIH3T3 cells into

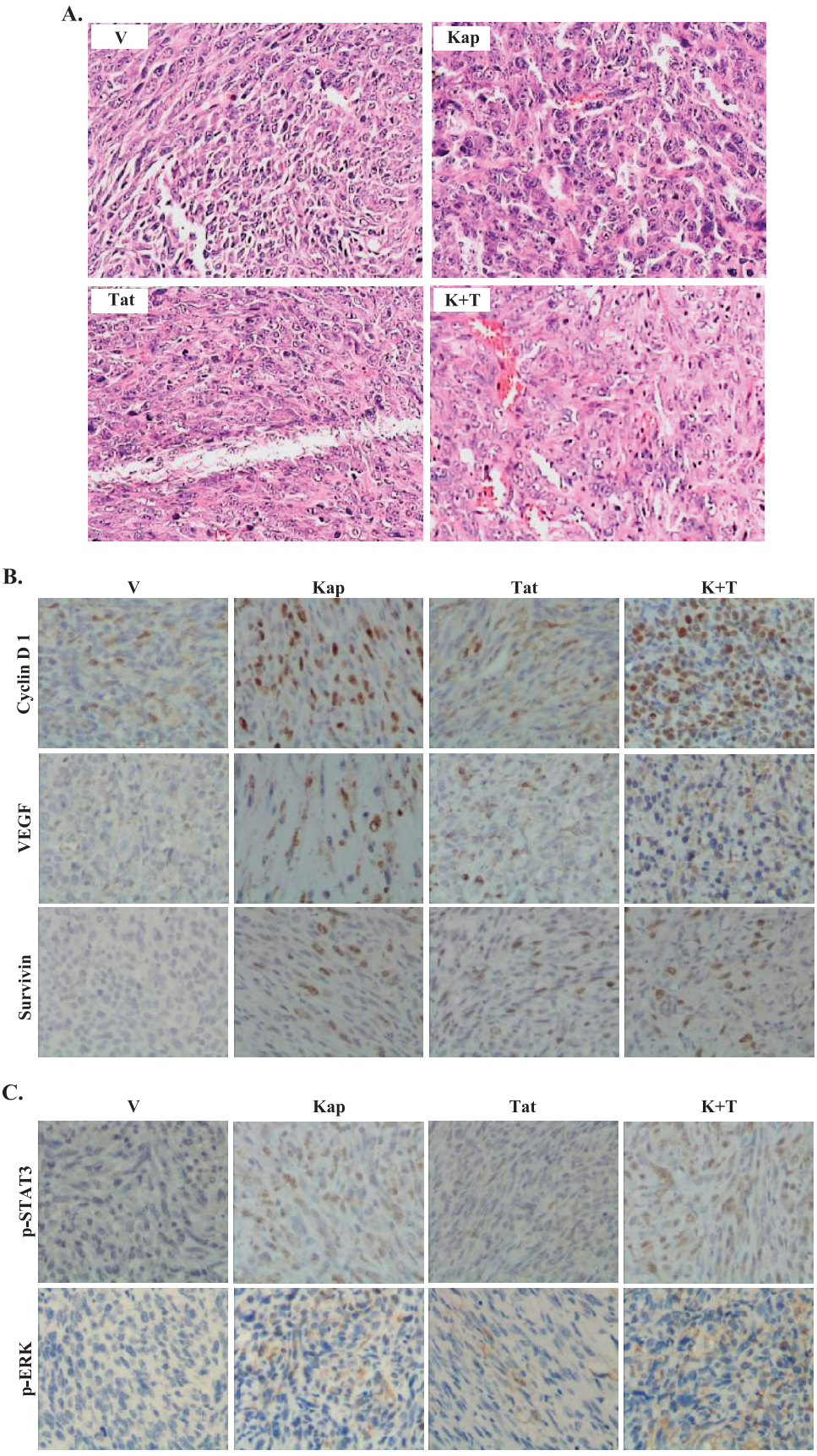
A.
V
Kap
Tat
K+T
B.
V
Kap
Tat
K+T
Cyclin D 1
VEGF
Survivin
C.
V
Kap
Tat
K+T
p-STAT3
p-ERK

nude mice for each construct. Mice were observed every day for the appearance of tumors at the site of injection, and tumors were measured in two dimensions after they first became visible. As shown in Figure 3*A*, tumors in three of the mice receiving cells transfected with Kaposin A plus Tat construct were detectable by day 9 after inoculation. The earliest appearance of a tumor in the Kaposin A group was at day 14, by which time all mice from the Kaposin A plus Tat group had detectable tumor. And only three of five nude mice for Tat construct had detectable tumors at day 30, and the earliest appearance of a tumor in the Tat group was at day 17 after inoculation. As judged from the volume of the tumor, the tumor growth rate was strikingly higher with the Kaposin A plus Tat group compared with rates for Kaposin A, Tat, and control. The data are summarized in Figure 3*B*. Tumors were removed at day 30, weighted and sectioned for further analysis. Three tumors in mice injected with the control vector weighed 0.07 ± 0.09 g, and three in the Tat group weighed 0.13 ± 0.13 g. The Kaposin A group had an average weight of 0.39 ± 0.20 g and Kaposin A plus Tat group weighed 5.64 ± 1.71 g (Figure 3*C*). Representative mice from four different groups at day 30 after inoculation showed typical tumors in Figure 3*D*. Taken together, these data suggest that Tat may accelerate and enhance tumorigenesis by Kaposin A in nude mice.

Histologically, Kaposin A–transfected NIH3T3 cells induced high-grade undifferentiated sarcomas, which was consistent with the previous report [17]. The tumor was characterized by hemorrhagic necrotic foci, which was different in size and irregular in shape. Numerous multinucleate huge cells, newly formed vessels, and scattered lymphocytes were seen in tumor sections (Figure 4*A*). Similar features were also observed in the tumor induced by Kaposin A plus Tat–transfected NIH3T3 cells. However, tumor necrosis range was more distinguishable, and more multinucleate huge cells, newly formed vessels, and infiltration lymphocytes were found in Kaposin A plus Tat–induced tumor (Figure 4*A*). Immunohistochemical staining demonstrated that expression levels of cyclin D1, VEGF, and Survivin in tumor tissue from mice of Kaposin A group were higher than those of vector and Tat groups (Figure 4*B*). Similarly, expressions of these three proteins in tumor tissue from of Kaposin A plus Tat mouse were elevated compared with vector and Tat groups and slightly increased compared with Kaposin A group (Figure 4*B*). These data suggest that Tat may increase expressions of cyclin D1, VEGF, and Survivin by Kaposin A in mouse tumor tissues.

Again, the Q Series signal transduction gene array in mouse cancer was used to detect the potential signal pathway(s) in tumor tissues. As shown in Table 2, mRNA of many gene indicators for the activation of 15 different signal pathways in Kaposin A, Tat, and Kaposin A plus Tat–induced tumor tissue were also altered to some degree compared with control vector–induced tumor tissue. Because Tat increased the activation of the MEK/ERK, STAT3, and PI3K/Akt signals in Kaposin A–transduced NIH3T3 cells (Figure 2, *A*–*C*), we further tried to detect phosphorylation of these molecules in the tumor tissue. Figure 4*C* demonstrated that phosphorylation levels of STAT3 and ERK in Kaposin A–induced tumor tissue were higher than vector and Tat groups. Phosphorylation levels of these two proteins in tumor tissue from Kaposin A plus Tat mouse were also elevated compared with those from vector and Tat groups and slightly increased compared with those from Kaposin A group (Figure 4*C*). Together, these data suggest that multiple signaling are likely involved in Tat-enhanced tumorigenesis by Kaposin A.

Activation of STAT3 Partially Contributes to Tumorigenesis by Kaposin A

STAT3 activation has been shown to enhance oncogenic potential of multiple viruses such as Epstein-Barr virus, human T-cell lymphotropic virus 1, and herpesvirus Saimiri [30–32]. Strong activation of STAT3 by Tat in Kaposin A–transduced cells suggests that STAT3 pathway may be involved in tumorigenesis by Kaposin A or Kaposin A plus Tat. To test this hypothesis, we first transiently transfected Kaposin A and Kaposin A plus Tat transfectants with STAT3-DN construct or pMSCV vector (the STAT3-DN construct was cloned in pMSCV vector), respectively, and then injected these cells into nude mice. As described previously, mice were observed, and the tumors were measured in two dimensions after they first became visible. Interestingly, we found that the tumor growth rate of Kaposin A + STAT3-DN group was much lower than that of Kaposin A + vector group (Figure 5). The earliest appearance of a tumor in the Kaposin A + STAT3-DN group was at day 15 after inoculation, but Kaposin A + vector group was at day 12. However, we did not observe any difference in the tumor growth rate between Kaposin A plus Tat + STAT3-DN and Kaposin A plus Tat + vector groups (data not shown). These data suggest that activation of STAT3 may, at least in part, contribute to tumorigenesis by Kaposin A, not Kaposin A plus Tat.

Tat Also Accelerates Tumorigenesis by Kaposin A in Immunocompetent Mice

To determine whether Kaposin A, Tat, or Kaposin A plus Tat–induced tumors in nude mice can grow in immunocompetent mice, the tumors were minced, digested with 0.1% collagenase, and cultured in DMEM. G418-resistant cells were analyzed for Kaposin A and Tat expression by RT-PCR. It was demonstrated that Kaposin A mRNA was readily expressed in G418-resistant cells from Kaposin A and Kaposin A plus Tat–induced tumor tissues and Tat mRNA was also expressed in G418-resistant cells from Tat and Kaposin A plus Tat–induced tumor tissues (data not shown). The cells were then injected s.c. into the right flanks of BALB/c immunocompetent mice. The animals were monitored every day for the appearance of tumors. As shown

Figure 4. Hematoxylin-eosin and immunohistochemical staining for characteristic of tumor induced by Kaposin A and Tat (original magnification, ×400). (A) Representative microscopic appearance of tumor tissues. Tumors were induced by s.c. injection with the pcDNA3.1 vector– (V), Kaposin A– (Kap), Tat- (Tat), and Kaposin A plus Tat– (K + T) transfected NIH3T3 cells in nude mice and were formalin-fixed and paraffin-embedded in their entireties as described in Materials and Methods. Hematoxylin-eosin staining of representative tumor sections showed hemorrhagic tumor necrotic foci and abundance of blood vessels in a selected area of tumor tissue. (B) Immunohistochemical staining of cyclin D1, VEGF, and Survivin expressed in the tumor tissue from nude mice. Cyclin D1, VEGF, and Survivin expressed in the tumor tissue of mice induced by the pcDNA3.1 vector– (V), Kaposin A– (Kap), Tat- (Tat), and Kaposin A plus Tat– (K + T) transfected NIH3T3 cells. (C) Immunohistochemical staining of phosphorylated STAT3 and ERK expression in tumor tissue from nude mice. Phosphorylated STAT3 and ERK expressed in tumor tissue of mice induced by the pcDNA3.1 vector– (V), Kaposin A– (Kap), Tat- (Tat), and Kaposin A plus Tat– (K + T) transfected NIH3T3 cells.

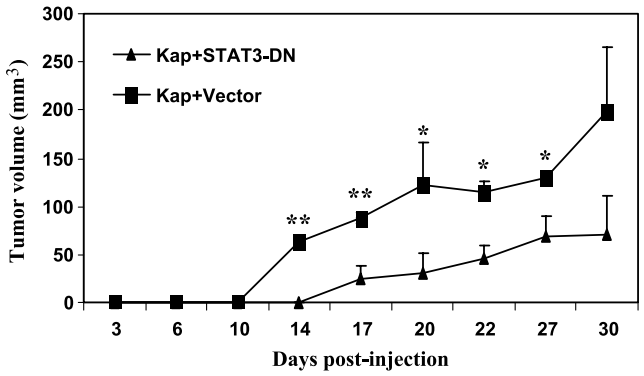

Figure 5. Activation of STAT3 partially contributes to tumorigenesis medicated by Kaposin A. Tumors were induced by s.c. injection with the Kaposin A–transfected NIH3T3 cells transiently transfected with STAT3-DN construct (Kap + STAT3-DN) or pMSCV vector (Kap + Vector) in nude mice as described in Materials and Methods. Plot of the volume of the tumors was drawn. The results are expressed as the mean ± SD ($n = 3$). $^{*}P < .05$ or $^{**}P < .01$ for Student's *t*-test *versus* Kap + STAT3-DN group.

in Figure 6*A*, tumors in 5 of 10 immunocompetent mice receiving cells from Kaposin A plus Tat–induced tumor in nude mice were detectable at day 14 after inoculation, and the earliest appearance of a tumor in this group was at day 8. Furthermore, tumors in 4 of 10 animals receiving cells from Tat-induced tumor were detectable at day 15 after inoculation, and the earliest appearance of a tumor in this group was at day 9. However, only 1 of 10 mice receiving cells from Kaposin A–induced tumor in nude mice developed tumor by day 17 after inoculation. Expectedly, none of immunocompetent mice receiving cells from control vector–induced tumor developed tumor by day 30 after inoculation (Figure 6*A*). As judged from the volume of the tumor, the tumor growth rate of Kaposin A plus Tat group was slightly higher than that of the Tat group. However, it was significantly higher than those of Kaposin A and control vector groups, which are summarized in Figure 6*B*. These data collectively suggest that Tat can also accelerate tumorigenesis mediated by Kaposin A in immunocompetent mice.

Discussion

The HIV-1 transactivator protein Tat has long been of particular interest to investigators studying AIDS-KS pathogenesis [5,33]. On one hand, Tat (including extracellular and intracellular Tat) suffices to reactivate latent KSHV by activation of JAK/STAT signaling [10,34]. Full-length Tat and a 13–amino acid peptide corresponding to the basic region of Tat can specifically enhance the entry of KSHV into endothelial and other cells, probably by concentrating virions on cell surface [35]. Conversely, Tat can act as a growth factor for KS-derived endothelial cells, enhance angiogenesis, and promote KS progression [4,5,8], possibly in part through synergy with or dysregulation of the expression of proinflammatory cytokines [6–9]. Furthermore, by inducing activation of NF-AT and NF-κB signals, Tat accelerates tumorigenesis by KSHV vGPCR *in vivo* [22]. These data suggest that Tat plays an important role in pathogenesis of AIDS-KS.

In this study, we investigated the potential of Tat to influence tumorigenesis induced by Kaposin A and explored the possible mechanisms by which Tat enhances Kaposin A–mediated tumorigenesis. Our experiments provide the direct experimental evidence that Tat not only enhances Kaposin A–induced NIH3T3 cells proliferation *in vitro* but also accelerates tumorigenesis by Kaposin A in *nu/nu* mice. Previous studies indicated that Kaposin A has multiple functions in single-gene transfer assays [17,36–38]. It can induce focus formation in Rat-3 cells and NIH3T3 cells and cause anchorage-independent growth and loss of contact inhibition in NIH3T3 cells. Rat-3 cells expressing Kaposin A are tumorigenic in *nu/nu* mice [17]. Here, we confirmed that Kaposin A has the ability to promote proliferation of NIH3T3 cells. When Tat was transfected into NIH3T3 cells expressing Kaposin A, it significantly enhanced Kaposin A–induced cell proliferation, suggesting that there is a molecular interaction between Tat and Kaposin A *in vitro*. Furthermore, when NIH3T3 cells coexpressing Kaposin A and Tat were injected into nude mice, the onset of tumor was earlier than those of NIH3T3 cells expressing Kaposin A or Tat alone. Meanwhile, its tumor growth rate was significantly faster, and the average weight was heavier than groups of Kaposin A or Tat alone, suggesting that intracellular Tat accelerates and enhances Kaposin A–induced tumorigenesis by an autocrine mechanism *in vivo*. KSHV is found in B lymphocytes, macrophages, keratinocytes, fibroblasts,

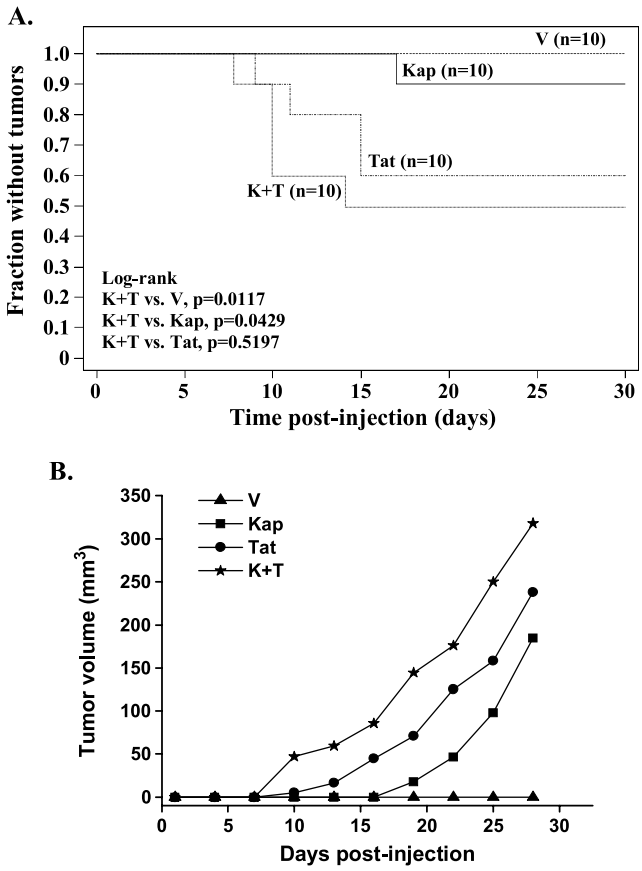

Figure 6. Tat accelerates tumorigenesis induced by Kaposin A in BALB/c immunocompetent mice. (A) A Kaplan-Meier plot for the time of appearance of palpable tumors is shown. Tumors were induced by s.c. injection with the cells derived from the pcDNA3.1 vector– (V), Kaposin A– (Kap), Tat- (Tat), and Kaposin A plus Tat– (K + T) induced tumor tissues in nude mice as described in Materials and Methods. A log-rank analysis gave *P* values of .0117 and .0429 for the comparison of K + T with control vector and Kaposin A, respectively. The log-rank *P* values were .5197 for the comparison of Tat with K + T and .1074 for the Kaposin A with Tat, indicating that there were no significant differences between these groups. (B) Plot of the volume of the tumors.

epithelial cells, KS tumor cells, and endothelial cells [39]. By contrast, the predominant host cells for HIV-1 are $CD4^+$ T lymphocytes, dendritic cells, and mononuclear phagocytes [40,41]. Although HIV-1 and KSHV generally do not infect the same cell, cells infected by the two viruses are often in close proximity. Tat is secreted from infected cells (namely, extracellular Tat) and can bind to both $\alpha_v\beta_3$ and $\alpha_5\beta_1$ integrins on the surface of target cells initiating intracellular signals that ultimately lead to changes in cellular gene expression [4,33]. Conversely, the extracellular Tat nonspecifically binds to cells membranes and is internalized [5,42]. Like intracellular Tat, this internalized Tat may directly interact with cellular genes to alter gene expression. Here, we just evaluated the potential of intracellular Tat to influence Kaposin A–mediated tumorigenesis. However, whether by a paracrine mechanism extracellular Tat may also have such function is still unknown.

In the current study, Tat was observed to enhance the proliferation of Kaposin A–transformed cells with both colony formation in soft agar and ^{3}H-TdR incorporation assays. Although cell cycle analysis showed a slightly increasing trend in S-phase of Kaposin A plus Tat transfectant, it did not seem to reveal a significant difference compared with Tat or Kaposin A alone. We pondered that the S-phase alone of cell cycle, which represents DNA synthesis ability, was not only one index for evaluation of cell proliferation. It was a complicated process and needed the multiplicity factors to be involved in. Furthermore, Tat drastically increased the MEK/ERK, STAT3, and PI3K/Akt signals by Kaposin A. With regard to signaling activated by Kaposin A, a previous study indicated that the transforming and adhesion effects of Kaposin A are mediated through its association with cytohesin-1, a guanine nucleotide exchange factor for ARF GTPases, which regulates integrin activity and is important for transformation [36]. In fact, a dominant-negative cytohesin-1–inhibited Kaposin A induced focus formation and restored normal actin organization. As for Tat, it can not only increase spindle cells viral load and expression of various viral genes with oncogenic potential (vGPCR, vBCL2, and viral interferon-regulatory factor 1) [11] but also activate multiple signaling pathways and has many functions on AIDS-KS pathogenesis. For instance, NF-AT and NF-κB signaling activated by KSHV vGPCR are synergistically increased by Tat and Tat can accelerate tumorigenesis induced by vGPCR. The effects of both vGPCR and Tat on signaling are dependent on the PI3K/Akt pathway [22,43]. Here, we found that Kaposin A alone upregulates phosphorylated Akt and STAT3, both of which are involved in cell proliferation and tumor formation [28,29,44]. Furthermore, Tat increases STAT3, PI3K/Akt, and MEK/ERK signaling activated by Kaposin A both *in vitro* and *in vivo*. Actually, the data from microarray demonstrated mRNA of many gene indicators for the activation of 15 different signal pathways in both cells and tumor tissues were altered to some degree. Therefore, our results did not eliminate the possibility that other pathway(s) may also be involved in Tat-accelerated tumorigenesis by Kaposin A.

In addition, we also found that Tat accelerated Kaposin A–medicated tumorigenesis in immunocompetent mice. Recent studies by Thirunarayanan et al. [45] reported that vGPCR-expressing cells established from tumors, which were induced with retrovirus-transduced vGPCR-expressing NIH3T3 cells in nude mice, gave rise to tumors in immunocompetent mice. Here, Kaposin A plus Tat-expressing cells established from tumors induced with Kaposin A plus Tat–expressing NIH3T3 cell lines in nude mice gave rise to tumors with 50% incidence. Unexpectedly, the tumor incidence of Kaposin A–expressing cells in immunocompetent mice was only 10%; however, Tat was 40%. Noteworthy, the time of tumor formation of Kaposin A plus Tat group was earlier, and tumor size was bigger than those of Kaposin A or Tat groups in immunocompetent mice. On one hand, rapid growth of subcutaneously injected Kaposin A plus Tat–expressing cells established from nude mice tumors in immunocompetent hosts probably was attributed to failure of the tumor cells to reach organized lymphoid organs resulting in the insufficient presentation of the tumor associated antigens [46]. Conversely, the ability of Kaposin and Tat–coexpressing NIH3T3 cells to survive immune surveillance could be a result of as yet unknown immunomodulatory effects of Tat, and also other molecular changes occurred during tumor progression.

In summary, we have shown that Tat could accelerate tumorigenesis induced by Kaposin A, and several signal pathways were involved in this process. Because both Tat and Kaposin A can activate multiple signaling pathways *in vitro* and *in vivo*, further studies are needed to understand which signal is a key signal to control Tat–accelerated tumorigenesis by Kaposin A *in vivo*.

Acknowledgments

The authors thank Z. Huang at Northwestern University Feinberg School of Medicine for critical reading of the manuscript and D. Link of the Washington University School of Medicine for plasmid pMSCV-STAT3D-EGFP.

References

[1] Chang Y, Cesarman E, Pessin MS, Lee F, Culpepper J, Knowles DM, and Moore PS (1994). Identification of herpesvirus-like DNA sequences in AIDS-associated Kaposi's sarcoma. *Science* **266**, 1865–1869.

[2] Biggar RJ, Rosenberg PS, and Cote T (1996). Kaposi's sarcoma and non–Hodgkin's lymphoma following the diagnosis of AIDS. Multistate AIDS/Cancer Match Study Group. *Int J Cancer* **68**, 754–758.

[3] Ariyoshi K, Schim van der Loeff M, Cook P, Whitby D, Corrah T, Jaffar S, Cham F, Sabally S, O'Donovan D, Weiss RA, et al. (1998). Kaposi's sarcoma in the Gambia, West Africa is less frequent in human immunodeficiency virus type 2 than in human immunodeficiency virus type 1 infection despite a high prevalence of human herpesvirus 8. *J Hum Virol* **1**, 193–199.

[4] Ensoli B, Barillari G, Salahuddin SZ, Gallo RC, and Wong-Staal F (1990). Tat protein of HIV-1 stimulates growth of cells derived from Kaposi's sarcoma lesions of AIDS patients. *Nature* **345**, 84–86.

[5] Ensoli B, Buonaguro L, Barillari G, Fiorelli V, Gendelman R, Morgan RA, Wingfield P, and Gallo RC (1993). Release, uptake, and effects of extracellular human immunodeficiency virus type 1 Tat protein on cell growth and viral transactivation. *J Virol* **67**, 277–287.

[6] Ensoli B, Gendelman R, Markham P, Fiorelli V, Colombini S, Raffeld M, Cafaro A, Chang HK, Brady JN, and Gallo RC (1994). Synergy between basic fibroblast growth factor and HIV-1 Tat protein in induction of Kaposi's sarcoma. *Nature* **371**, 674–680.

[7] Fiorelli V, Gendelman R, Samaniego F, Markham PD, and Ensoli B (1995). Cytokines from activated T cells induce normal endothelial cells to acquire the phenotypic and functional features of AIDS–Kaposi's sarcoma spindle cells. *J Clin Invest* **95**, 1723–1734.

[8] Barillari G, Sgadari C, Palladino C, Gendelman R, Caputo A, Morris CB, Nair BC, Markham P, Nel A, Sturzl M, et al. (1999). Inflammatory cytokines synergize with the HIV-1 Tat protein to promote angiogenesis and Kaposi's sarcoma via induction of basic fibroblast growth factor and the $\alpha_v\beta_3$ integrin. *J Immunol* **163**, 1929–1935.

[9] Buonaguro L, Barillari G, Chang HK, Bohan CA, Kao V, Morgan R, Gallo RC, and Ensoli B (1992). Effects of the human immunodeficiency virus type 1 Tat protein on the expression of inflammatory cytokines. *J Virol* **66**, 7159–7167.

[10] Zeng Y, Zhang X, Huang Z, Cheng L, Yao S, Qin D, Chen X, Tang Q, Lv Z, Zhang L, et al. (2007). Intracellular Tat of human immunodeficiency virus type 1 activates lytic cycle replication of Kaposi's sarcoma–associated herpesvirus: role of JAK/STAT signaling. *J Virol* **81**, 2401–2417.

[11] Pyakurel P, Pak F, Mwakigonja AR, Kaaya E, and Biberfeld P (2007). KSHV/HHV-8 and HIV infection in Kaposi's sarcoma development. *Infect Agent Cancer* **2**, 4.

[12] Tomkowicz B, Singh SP, Lai D, Singh A, Mahalingham S, Joseph J, Srivastava S, and Srinivasan A (2005). Mutational analysis reveals an essential role for the LXXLL motif in the transformation function of the human herpesvirus-8 oncoprotein, kaposin. *DNA Cell Biol* **24**, 10–20.

[13] Staskus KA, Zhong W, Gebhard K, Herndier B, Wang H, Renne R, Beneke J, Pudney J, Anderson DJ, Ganem D, et al. (1997). Kaposi's sarcoma–associated herpesvirus gene expression in endothelial (spindle) tumor cells. *J Virol* **71**, 715–719.

[14] Sturzl M, Blasig C, Schreier A, Neipel F, Hohenadl C, Cornali E, Ascherl G, Esser S, Brockmeyer NH, Ekman M, et al. (1997). Expression of HHV-8 latency-associated T0.7 RNA in spindle cells and endothelial cells of AIDS-associated, classical and African Kaposi's sarcoma. *Int J Cancer* **72**, 68–71.

[15] Linderoth J, Rambech E, and Dictor M (1999). Dominant human herpesvirus type 8 RNA transcripts in classical and AIDS-related Kaposi's sarcoma. *J Pathol* **187**, 582–587.

[16] Sadler R, Wu L, Forghani B, Renne R, Zhong W, Herndier B, and Ganem D (1999). A complex translational program generates multiple novel proteins from the latently expressed kaposin (K12) locus of Kaposi's sarcoma–associated herpesvirus. *J Virol* **73**, 5722–5730.

[17] Muralidhar S, Pumfery AM, Hassani M, Sadaie MR, Kishishita M, Brady JN, Doniger J, Medveczky P, and Rosenthal LJ (1998). Identification of kaposin (open reading frame K12) as a human herpesvirus 8 (Kaposi's sarcoma–associated herpesvirus) transforming gene. *J Virol* **72**, 4980–4988.

[18] Bais C, Santomasso B, Coso O, Arvanitakis L, Raaka EG, Gutkind JS, Asch AS, Cesarman E, Gershengorn MC, and Mesri EA (1998). G-protein–coupled receptor of Kaposi's sarcoma–associated herpesvirus is a viral oncogene and angiogenesis activator. *Nature* **391**, 86–89.

[19] Sodhi A, Montaner S, Patel V, Zohar M, Bais C, Mesri EA, and Gutkind JS (2000). The Kaposi's sarcoma–associated herpes virus G protein–coupled receptor up-regulates vascular endothelial growth factor expression and secretion through mitogen-activated protein kinase and p38 pathways acting on hypoxia-inducible factor 1α. *Cancer Res* **60**, 4873–4880.

[20] Yang TY, Chen SC, Leach MW, Manfra D, Homey B, Wiekowski M, Sullivan L, Jenh CH, Narula SK, Chensue SW, et al. (2000). Transgenic expression of the chemokine receptor encoded by human herpesvirus 8 induces an angioproliferative disease resembling Kaposi's sarcoma. *J Exp Med* **191**, 445–454.

[21] Guo HG, Sadowska M, Reid W, Tschachler E, Hayward G, and Reitz M (2003). Kaposi's sarcoma–like tumors in a human herpesvirus 8 ORF74 transgenic mouse. *J Virol* **77**, 2631–2639.

[22] Guo HG, Pati S, Sadowska M, Charurat M, and Reitz M (2004). Tumorigenesis by human herpesvirus 8 vGPCR is accelerated by human immunodeficiency virus type 1 Tat. *J Virol* **78**, 9336–9342.

[23] McLemore ML, Grewal S, Liu F, Archambault A, Poursine-Laurent J, Haug J, and Link DC (2001). STAT-3 activation is required for normal G-CSF–dependent proliferation and granulocytic differentiation. *Immunity* **14**, 193–204.

[24] Lu C, Zeng Y, Huang Z, Huang L, Qian C, Tang G, and Qin D (2005). Human herpesvirus 6 activates lytic cycle replication of Kaposi's sarcoma–associated herpesvirus. *Am J Pathol* **166**, 173–183.

[25] Qin D, Zeng Y, Qian C, Huang Z, Lv Z, Cheng L, Yao S, Tang Q, Chen X, and Lu C (2008). Induction of lytic cycle replication of Kaposi's sarcoma–associated herpesvirus by herpes simplex virus type 1: involvement of IL-10 and IL-4. *Cell Microbiol* **10**, 713–728.

[26] Yao S, Tang Q, Cheng L, Zeng Y, Chen X, Qin D, Lv Z, and Lu C (2007). Identification of B cell epitopes at the C-terminus of latency-associated nuclear protein of the Kaposi's sarcoma–associated herpesvirus. *Acta Virol* **51**, 109–118.

[27] Kolble K, Ullrich OM, Pidde H, Barthel B, Diermann J, Rudolph B, Dietel M, Schlag PM, and Scherneck S (1999). Microsatellite alterations in serum DNA of patients with colorectal cancer. *Lab Invest* **79**, 1145–1150.

[28] Kim D, Cheng GZ, Lindsley CW, Yang H, and Cheng JQ (2005). Targeting the phosphatidylinositol-3 kinase/Akt pathway for the treatment of cancer. *Curr Opin Investig Drugs* **6**, 1250–1258.

[29] Luo J, Manning BD, and Cantley LC (2003). Targeting the PI3K-Akt pathway in human cancer: rationale and promise. *Cancer Cell* **4**, 257–262.

[30] Lund TC, Garcia R, Medveczky MM, Jove R, and Medveczky PG (1997). Activation of STAT transcription factors by herpesvirus Saimiri Tip-484 requires $p56^{lck}$. *J Virol* **71**, 6677–6682.

[31] Migone TS, Lin JX, Cereseto A, Mulloy JC, O'Shea JJ, Franchini G, and Leonard WJ (1995). Constitutively activated Jak-STAT pathway in T cells transformed with HTLV-I. *Science* **269**, 79–81.

[32] Chen H, Hutt-Fletcher L, Cao L, and Hayward SD (2003). A positive autoregulatory loop of LMP1 expression and STAT activation in epithelial cells latently infected with Epstein-Barr virus. *J Virol* **77**, 4139–4148.

[33] Barillari G, Gendelman R, Gallo RC, and Ensoli B (1993). The Tat protein of human immunodeficiency virus type 1, a growth factor for AIDS Kaposi sarcoma and cytokine-activated vascular cells, induces adhesion of the same cell types by using integrin receptors recognizing the RGD amino acid sequence. *Proc Natl Acad Sci USA* **90**, 7941–7945.

[34] Harrington W Jr, Sieczkowski L, Sosa C, Chan-a-Sue S, Cai JP, Cabral L, and Wood C (1997). Activation of HHV-8 by HIV-1 tat. *Lancet* **349**, 774–775.

[35] Aoki Y and Tosato G (2004). HIV-1 Tat enhances Kaposi sarcoma–associated herpesvirus (KSHV) infectivity. *Blood* **104**, 810–814.

[36] Kliche S, Nagel W, Kremmer E, Atzler C, Ege A, Knorr T, Koszinowski U, Kolanus W, and Haas J (2001). Signaling by human herpesvirus 8 kaposin A through direct membrane recruitment of cytohesin-1. *Mol Cell* **7**, 833–843.

[37] Muralidhar S, Veytsmann G, Chandran B, Ablashi D, Doniger J, and Rosenthal LJ (2000). Characterization of the human herpesvirus 8 (Kaposi's sarcoma–associated herpesvirus) oncogene, kaposin (ORF K12). *J Clin Virol* **16**, 203–213.

[38] Tomkowicz B, Singh SP, Cartas M, and Srinivasan A (2002). Human herpesvirus-8 encoded Kaposin: subcellular localization using immunofluorescence and biochemical approaches. *DNA Cell Biol* **21**, 151–162.

[39] Blauvelt A (1999). The role of human herpesvirus 8 in the pathogenesis of Kaposi's sarcoma. *Adv Dermatol* **14**, 167–206; discussion 207.

[40] Martin JC and Bandres JC (1999). Cells of the monocyte-macrophage lineage and pathogenesis of HIV-1 infection. *J Acquir Immune Defic Syndr* **22**, 413–429.

[41] Weiss RA (2000). Getting to know HIV. *Trop Med Int Health* **5**, A10–A15.

[42] Selby MJ, Bain ES, Luciw PA, and Peterlin BM (1989). Structure, sequence, and position of the stem-loop in tar determine transcriptional elongation by tat through the HIV-1 long terminal repeat. *Genes Dev* **3**, 547–558.

[43] Pati S, Foulke JS Jr, Barabitskaya O, Kim J, Nair BC, Hone D, Smart J, Feldman RA, and Reitz M (2003). Human herpesvirus 8–encoded vGPCR activates nuclear factor of activated T cells and collaborates with human immunodeficiency virus type 1 Tat. *J Virol* **77**, 5759–5773.

[44] Heinrich PC, Behrmann I, Muller-Newen G, Schaper F, and Graeve L (1998). Interleukin-6-type cytokine signalling through the gp130/Jak/STAT pathway. *Biochem J* **334** (Pt 2), 297–314.

[45] Thirunarayanan N, Cifire F, Fichtner I, Posner S, Benga J, Reiterer P, Kremmer E, Kolble K, and Lipp M (2007). Enhanced tumorigenicity of fibroblasts transformed with human herpesvirus 8 chemokine receptor vGPCR by successive passage in nude and immunocompetent mice. *Oncogene* **26**, 5702–5712.

[46] Ochsenbein AF, Sierro S, Odermatt B, Pericin M, Karrer U, Hermans J, Hemmi S, Hengartner H, and Zinkernagel RM (2001). Roles of tumour localization, second signals and cross priming in cytotoxic T-cell induction. *Nature* **411**, 1058–1064.